Paleoceanography and Paleoclimatology

RESEARCH ARTICLE
10.1029/2019PA003674

Special Section:
Special Collection to Honor the Career of Robert C. Thunell

CO_2 Release From Pockmarks on the Chatham Rise-Bounty Trough at the Glacial Termination

Lowell Stott[1], Bryan Davy[2], Jun Shao[1], Richard Coffin[3], Ingo Pecher[4], Helen Neil[5], Paula Rose[3], and Joerg Bialas[6]

[1]Department of Earth Sciences, University of Southern California, Los Angeles, CA, USA, [2]Department of Marine Geosciences, GNS Science, Lower Hutt, New Zealand, [3]Department of Physical and Environmental Sciences, Texas A&M University-Corpus Christi, Corpus Christi, TX, USA, [4]School of Environment, University of Auckland, Auckland, New Zealand, [5]National Institute of Water & Atmospheric Research Ltd (NIWA), Wellington, New Zealand, [6]GEOMAR Helmholtz-Centre for Ocean Research Kiel, Kiel, Germany

Key Points:
- Pockmarks of varying size occur across a vast portion of the Chatham Rise and Bounty Trough in the Southwest Pacific
- Pockmarks overlie subsurface deformation features indicative of overpressurized vertical fluid flow
- Negative $\Delta^{14}C$ nomalies occur near pockmarks indicating these were where ^{14}C-dead carbon was released to the ocean at the last glacial termination

Supporting Information:
- Supporting Information S1

Correspondence to:
L. Stott,
stott@usc.edu

Citation:
Stott, L., Davy, B., Shao, J., Coffin, R., Pecher, I., Neil, H., et al. (2019). CO_2 Release From Pockmarks on the Chatham Rise-Bounty Trough at the Glacial Termination. *Paleoceanography and Paleoclimatology*, *34*, 1726–1743. https://doi.org/10.1029/2019PA003674

Received 29 MAY 2019
Accepted 18 SEP 2019
Accepted article online 19 OCT 2019
Published online 14 NOV 2019

Abstract Seafloor pockmarks of varying size occur over an area of 50,000 km^2 on the Chatham Rise, Canterbury Shelf and Inner Bounty Trough, New Zealand. The pockmarks are concentrated above the flat-subducted Hikurangi Plateau. Echosounder data identify recurrent episodes of pockmark formation at ~100,000-year frequency coinciding with Pleistocene glacial terminations. Here we show that there are structural conduits beneath the larger pockmarks through which fluids flowed upward toward the seafloor. Large negative $\Delta^{14}C$ excursions are documented in marine sediments deposited next to these subseafloor conduits and pockmarks at the last glacial termination. Modern pore waters contain no methane, and there is no negative $\delta^{13}C$ excursion at the glacial termination that would be indicative of methane or mantle-derived carbon at the time the $\Delta^{14}C$ excursion and pockmarks were produced. An ocean general circulation model equipped with isotope tracers is unable to simulate these large $\Delta^{14}C$ excursions on the Chatham Rise by transport of hydrothermal carbon released from the East Pacific Rise as previous studies suggested. Here we attribute the $\Delta^{14}C$ anomalies and pockmarks to release of ^{14}C-dead CO_2 and carbon-rich fluids from subsurface reservoirs, the most likely being dissociated Mesozoic carbonates that subducted beneath the Rise during the Late Cretaceous. Because of the large number of pockmarks and duration of the $\Delta^{14}C$ anomaly, the pockmarks may collectively represent an important source of ^{14}C-dead carbon to the ocean during glacial terminations.

1. Introduction

One of the challenges in Ocean and Climate Science is to learn what Earth System processes contributed to the variations in atmospheric pCO_2 that accompanied each glacial cycle of the late Pleistocene. It is particularly striking that each glacial/interglacial cycle during the late Pleistocene was characterized by a long decline of atmospheric pCO_2 that spanned ~100,000 years but glacial terminations were accompanied by a much more rapid rise in pCO_2. This puzzling temporal asymmetry at the glacial terminations does not match the slow varying changes in solar insolation that seemingly paced glacial cycles at 100,000-year frequency during the late Pleistocene. The saw-toothed shape to glacial cycles and their accompanying changes in atmospheric pCO_2 (Petit et al., 1999) require there to be regulatory mechanisms within the carbon and climate systems that produce theses abrupt transitions.

The leading hypothesis to explain the glacial pCO_2 cycles calls for reduced ocean ventilation during glaciations and accumulation of respired metabolic carbon somewhere in the deep sea (Toggweiler, 1999), followed by rapid ventilation of that stored carbon at glacial terminations, perhaps in response to weakening of the Atlantic Meridional Overturning Circulation. In models, a weakened Atlantic Meridional Overturning Circulation is associated with net transfer of energy from the Northern Hemisphere to the Southern Hemisphere. The net transfer of excess energy to the Southern Hemisphere leads to a reduction of sea ice around the Southern Ocean and perhaps stronger westerly winds (Menviel et al., 2018). The intensification of the westerly winds is key to this hypothesis because it is thought to enhance Ekman pumping and upwelling of deep waters carrying excess carbon to the Southern Ocean (Anderson et al., 2009). But after three decades of scientific inquiry, there is still debate about how much excess respired carbon accumulated in the deep-sea during glaciations. There is evidence that the abyssal ocean was more stratified during the

Last Glacial Maximum (LGM; Adkins et al., 2002; Adkins & Schrag, 2003; Adkins, 2013; Basak et al., 2018; Burke & Robinson, 2012). But these reconstructions do not constrain the rate of ventilation during glacial cycles nor do these records constrain the extent to which the deep ocean sequestered additional carbon during glaciations. In fact, radiocarbon measurements from the deep Pacific that span the last glacial maxima do not provide unequivocal evidence that the deep ocean was less ventilated (Broecker et al., 2004; Broecker et al., 2008; Keigwin & Lehman, 2015; Lund et al., 2011). In a recent assessment of available radiocarbon data from the deep ocean, Zhao et al. (2018) concluded that deep water $\Delta^{14}C$ records do not require basin-scale changes in ventilation rate that would be different from modern, provided there were changes in surface reservoir ages that accompanied the deglaciation. Their study did not preclude the possibility of ventilation rate changes but instead points to the limits of using the available ^{14}C data alone to infer that there were changes in ventilation rate. In another recent study of Neodymium isotope data from the deep Pacific, Hu and Piotrowski (2018) concluded that overturning circulation was actually faster during the glacial relative to the Holocene.

At the same time, there have been recent studies that document large negative excursions in radiocarbon activity ($\Delta^{14}C$) at the last glacial termination (Bryan et al., 2010; Mangini et al., 2010; Marchitto et al., 2007; Ronge et al., 2016; Skinner et al., 2010; Stott et al., 2009, 2019). The spatial and temporal extent of these excursions have not yet been fully constrained, but they are not representative of the ocean's ^{14}C distribution (Zhao et al., 2018). These $\Delta^{14}C$ excursions have thus far been identified at intermediate water depths in the Atlantic, Pacific, and Indian Oceans (Bryan et al., 2010; Mangini et al., 2010; Rafter et al., 2018; Sikes et al., 2000; Stott et al., 2009, 2019) and in deeper waters in the south Atlantic (Skinner et al., 2010) and south Pacific, including sites on the Chatham Rise (Ronge et al., 2016). Some studies have called upon these ^{14}C age anomalies as evidence for the release of "old" respired carbon from a formally isolated deep ocean water mass (Bryan et al., 2010; Marchitto et al., 2007; Skinner et al., 2010). Stott and Timmermann (2011) questioned this however, pointing out that the magnitude of the $\Delta^{14}C$ excursions in the Eastern Equatorial Pacific are far too large to be indicative of actual ventilation ages. Instead, these excursions are hypothesized to have come from release of geologic carbon from hydrothermal systems nearby (Stott et al., 2019; Stott & Timmermann, 2011), possibly released when temperatures rose and destabilized the CO_2 reservoirs. Other studies have considered ways for geologic systems to influence carbon cycling on glacial timescales (Broecker et al., 2015; Huybers & Langmuir, 2017; Lund & Asimow, 2011; Ronge et al., 2016). But testing any of these hypotheses is difficult because the observational database is sparse, and the radiocarbon anomalies may involve more than one process. In the present study we present evidence that large $\Delta^{14}C$ anomalies observed in the southwest Pacific on Chatham Rise and Bounty Trough were produced by the release of ^{14}C-dead carbon to the ocean during the LGM and deglaciation through sea floor pockmarks that overlie subsurface deformation features that are indicative of overpressured sediments that would have acted as fluid conduits. The radiocarbon anomalies on Chatham Rise and Bounty Trough are found in biogenic sediments deposited directly adjacent to the large pockmarks that occur over a vast portion of the southwestern Chatham Rise and the Bounty Trough (Figure 1). Seismic evidence indicates pockmarks have formed repeatedly during the Pleistocene at a regular recurrence frequency (Davy et al., 2010).

Pockmarks are found on other continental margins as well (Hovland & Judd, 1988). At some of these sites, modern pore water geochemistry has been analyzed and found to contain large amounts of methane (Andreassen et al., 2017; Böttner et al., 2019; Feldens et al., 2016) implying that destabilization of methane clathrates at depth resulted in a release of methane that caused the deformation. But at other sites, it is less clear what the source of subsurface gas is because direct geochemical measurements from the pockmarks themselves are not available (e.g., de Mahiques et al., 2017; Somoza et al., 2014). In other coastal settings, seafloor deformation has been directly attributed to release of He and CO_2 gas from volcanic magmas (Passaro et al., 2016). In the present study we show that on the Chatham Rise, geochemical and isotope evidence points to CO_2 rather than CH_4 as the primary gas source responsible for the pockmarks. The most likely source of CO_2 would be from dissociated limestones that subducted beneath the Rise during the Late Cretaceous. Our study is an initial step in testing the hypothesis that deep sources of CO_2 beneath the Chatham Rise have been released during glacial terminations throughout the late Pleistocene and contributed to the systematic variations in atmospheric pCO_2 that accompanied glacial cycles. If ultimately validated, this hypothesis means that the Chatham Rise acted as carbon capacitor, accumulating carbon during glaciations and releasing carbon to the ocean during glacial terminations.

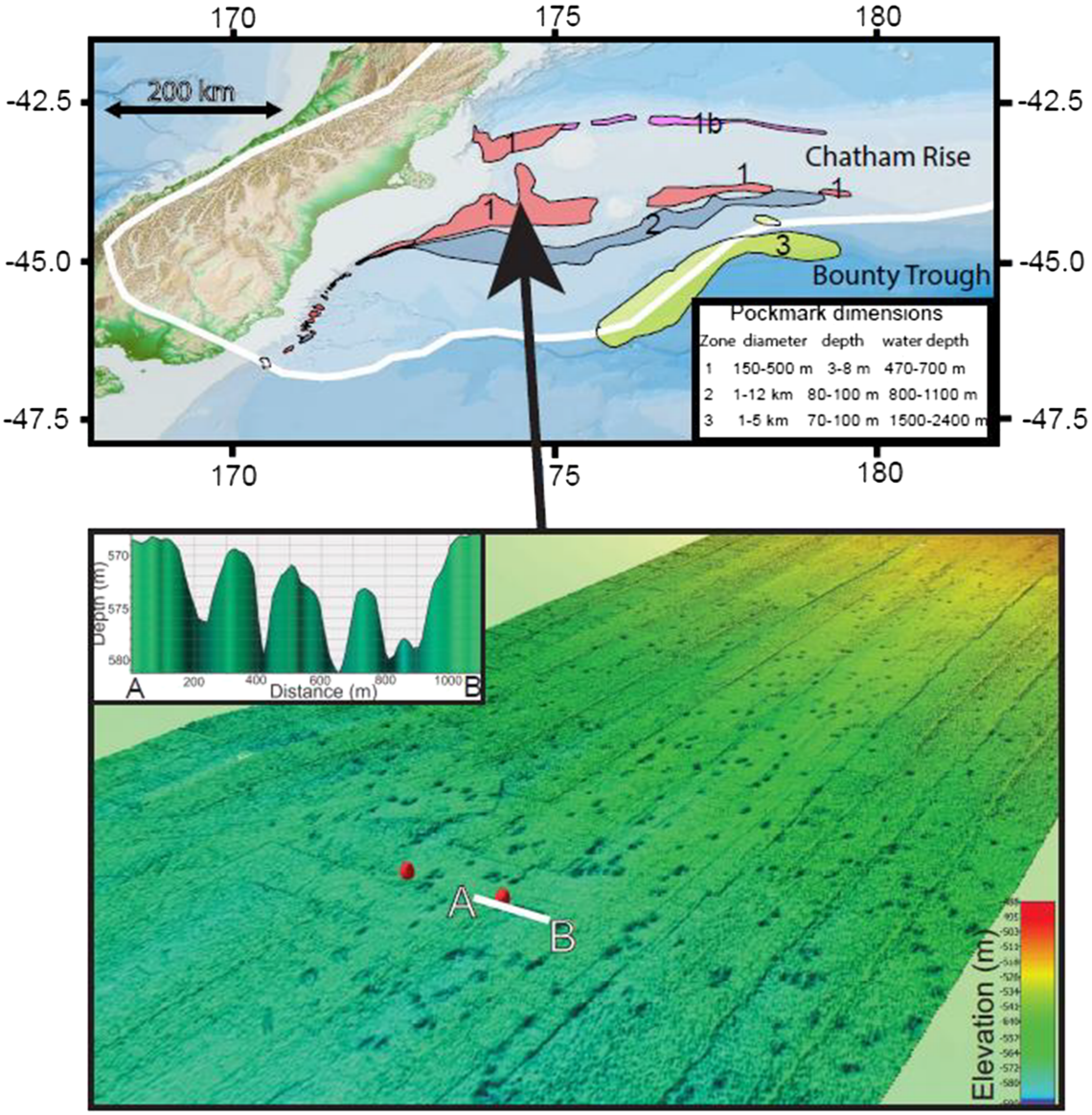

Figure 1. Upper panel depicts zones where pockmarks of varying size and depth occur across the Chatham Rise and Bounty Trough. Note that the largest pockmarks occur in the Bounty Trough. The lower panel is a section from Zone 1 illustrating the numerous small pockmarks exposed at the surface. The line A-B (inset) is a section across the smaller pockmarks. The red dots mark locations where piston cores were collected in 2013.

Table 1
Cores Used in this Study

Core	Long.	Lat.	Depth (m)	Author
PS75-104-1	−185.5	−44.77	835	Ronge et al. (2016)
SO213-84-1	−185.4	−45.13	972	Ronge et al. (2016)
PS75-100-4	−182.9	−45.76	2,498	Ronge et al. (2016)
SO213-82-1	−183.4	−45.78	2,066	Ronge et al. (2016)
U938	−180.5	−45.1	2,700	Sikes et al. (2000)
PC75-1,2	−182	−44.24	967	This paper

2. Materials and Methods

2.1. SO226 Leg 1, R/V Sonne Geophysical Survey

In an earlier study, Davy et al. (2010) hypothesized that the pockmarks that spread across the southwestern Chatham Rise were produced by seafloor methane venting from disassociated methane hydrate during glacial terminations. That hypothesis led to a two-leg geophysical and geochemical survey across the southern portion of Chatham Rise in 2013 (R/V Sonne Cruise SO226). Leg 1 of the SO226 Sonne survey undertook a combination of low-fold seismic reflection profiling and 3-D *P* cable seismic surveying (at two large pockmark sites). OBS data were collected for velocity control. The survey also collected Parasound subbottom seismic data and multibeam data for seafloor mapping (Table 1).

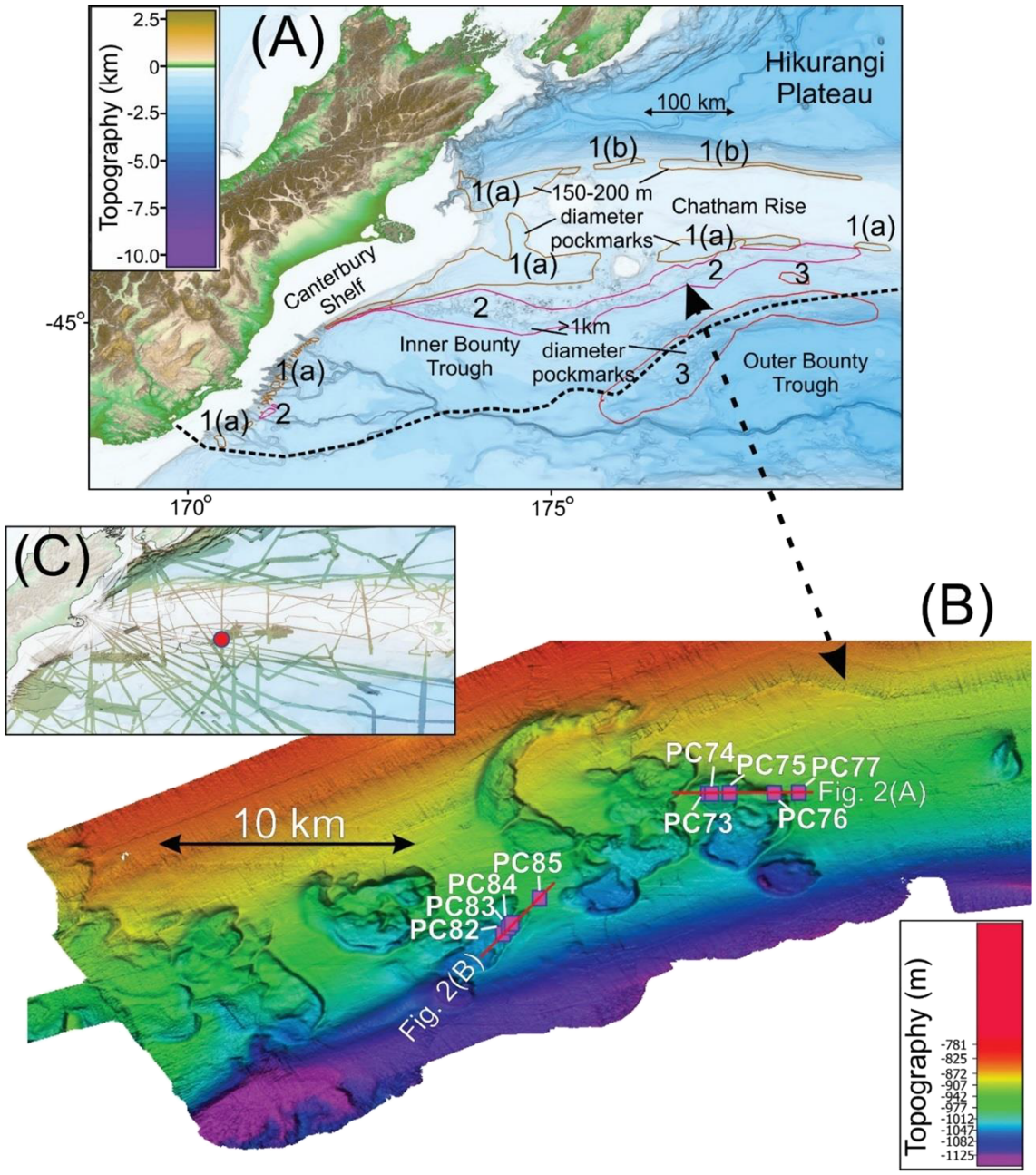

Figure 2. Upper panel (A), location of pockmarks over bathymetry (courtesy of NIWA). Heavy dashed line marks the interpreted southern extent of Hikurangi Plateau flat-subduction (Davy, 2014). Lower panel (B) multibeam bathymetry image from survey SO226 with core locations (red boxes). Red dot in panel (C) shows the profile lines and the location (red dot) of the pockmarks and cores shown in panel (B). Red dot in panel (C) covers the extent of panel (B).

2.2. SO226 Leg 2, R/V Sonne Coring and Geochemical Survey

Coring operations during SO226 Leg 2 targeted sites identified using seismic data from Leg 1 and included both piston and multi coring (Figure 2). Multicores were between 8 and 42 cm long and were sectioned at 1-cm intervals. Each core was split into ~25 sections at 10- **to** 40-cm intervals and capped. Porewater was extracted from each section using rhizon samplers (Dickens et al., 2007). Porewaters were extracted onboard for analysis of sulfide, sulfate, chloride, and dissolved inorganic carbon (DIC) concentrations. Samples were also preserved for stable carbon isotope ratios of DIC (Coffin et al., 2014). The onboard porewateranalysis was used to assess whether there is a modern flux of methane affecting the pore water chemistry.

For radiocarbon isotope analysis, background radiocarbon shipboard wipe tests were conducted to determine levels of radiocarbon present in laboratories, work, and storage areas and in the portable lab van (Coffin, Rose, et al., 2013). The Piston Core PC75 $\Delta^{14}C$ and stable isotope data are from Shao et al. (2019). The bulk sediment ^{14}C ages for Piston Cores PC45 and PC54 were generated at the Rafter AMS lab in New Zealand (supporting information Table S1). For radiocarbon isotope analysis of bulk sediment carbonate, CO_2 was generated by acidification and sealed tube (Coffin et al., 2015). Sample and data processing are as described by Stuiver and Polach (1977). The blank corrected, fraction modern was normalized to $\delta^{13}C = -25‰$ defined by Donahue et al. (1990). Stable carbon isotope analyses were combined with radiocarbon data to assess if there has been methane oxidation (Coffin et al., 2015). Stable oxygen and carbon isotope data from foraminifers from Piston Core PC75 are from Shao et al. (2019).

2.3. Age Modeling and $\Delta^{14}C$ Reconstructions

We recalculated $\Delta^{14}C$ for the Ronge et al. (2016) cores, PS75-100-4 and SO213-82-1 from the Bounty Trough as well as the PS75-104 and SO213-84-1 cores from the Chatham Rise based on a new age model developed using BChron. We did this so that all of the core chronologies are derived using the same calibration curve (MARINE13). For the late glacial and early deglacial sections, we adopted their surface reservoir ages because they are within ~300 years of that used by Shao et al. (2019). There is one exception; in Ronge et al.'s "tuned" age model for the PS75-104-1 core, the authors estimated a surface reservoir age of 243 years at 96 cm (15,435 ^{14}C age). We are not able to assess how robust either reservoir age is for this time interval. But importantly, in the early deglacial and late glacial portions of both cores, the $\Delta^{14}C$ estimates are in close agreement, and both cores document large negative $\Delta^{14}C$ excursions at shallow intermediate water depth on the Chatham Rise (Figure 5). The estimated uncertainties arising from both the $\Delta^{14}C$ estimates and age uncertainties are plotted as slanted quivers.

2.4. Earth System Modeling

The cGENIE model includes a 3-D dynamical ocean model coupled to the 2-D energy-moisture balance atmospheric model (Edwards & Marsh, 2005). The ocean model is based on a 36 × 36 horizontal grid with 16 vertical layers. cGENIE has a dynamic and thermodynamic component of sea ice. The model also incorporates a marine biogeochemical cycling of carbon and other tracers (Ridgwell et al., 2007). cGENIE simulations were first run under preindustrial conditions (Cao et al., 2009) for 10,000 years, with prescribed atmospheric $pCO_2 = 278$ ppm and atmospheric $\Delta^{14}C = -1‰$. Then the model was further spun up for 50,000 years with an atmospheric ^{14}C production rate of to 350 mol/year, equivalent to 1.3 atoms/cm^2/s. The atm $\Delta^{14}C$ could evolve freely at this stage. At the end of 50,000 years, atmospheric $\Delta^{14}C = 0.8‰$. The spin-up is not an attempt to reproduce the atmospheric radiocarbon condition at ~30 kyr BP, when Ronge et al. (2016) hypothesized mantle-sourced carbon was released into the South Pacific. For example, a production rate of 1.3 atoms/cm^2/s that we used is much smaller rather than ~2.2 atoms/cm^2/s from a recent reconstruction (Hain et al., 2014). This is mainly because the total carbon inventory in the atmosphere-ocean system in cGENIE is ~36,000 PgC and the bulk $\Delta^{14}C$ at equilibrium is −180‰, while in the calculation by Hain et al. (2014), the total carbon inventory is 43,000 PgC and bulk $\Delta^{14}C$ is ~0‰ at 30 kyr BP. The smaller total carbon inventory and more negative bulk $\Delta^{14}C$ in our spin up leads to a smaller ^{14}C rate compared to Hain et al. (2014) and, therefore, requires a smaller production rate at equilibrium. Nonetheless, our goal here is to achieve an ocean and atmosphere ^{14}C field that is in equilibrium with the prescribed ^{14}C production rate and therefore we can be sure that the ^{14}C response in the sensitivity experiments is not caused by the ^{14}C production rate in the atmosphere. In the DIC injection experiments, atmospheric ^{14}C production was held constant. The rationale for this is that there is no trend in the reconstructed atmospheric ^{14}C production rate between 30 and 20 kyr BP (Hain et al., 2014).

In each sensitivity experiment, a brine rejection process was turned on in cGENIE. The brine rejection is a simple parameterization of the sink of very salty water in the Southern Ocean during sea ice formation. The strength of this mechanism is represented by the "frac" parameter in cGENIE. The "frac" parameter is the proportion of the rejected salt that sinks to the abyss in the Southern Ocean. The higher the "frac," the denser and thus more stratified the deep ocean becomes. A "frac" value of 0.6 was chosen, falling in the range of a previous work that attempted to fit the simulated deep ocean radiocarbon to the reconstructions using the CLIMBER-2 model (Mariotti et al., 2013).

For injections of 0.16, 0.32, 0.64, and 1.28 GtC/year over 10,000 years, the total amount of carbon released is 1,600, 3,200, 6,400, and 12,800 GtC, respectively. This extra carbon would have a significant effect on the Earth's radiation budget and, consequently, a strong influence on the simulated climate. To compare the direct $\Delta\Delta^{14}C$ response driven by different injection rates in these sensitivity experiments, we therefore fixed the radiative forcing in all simulations to be 60% of the preindustrial level (i.e., LGM-like). Again, the purpose is to assess how the radiocarbon anomalies are manifest in the ocean in response to a release of carbon from the East Pacific Rise (EPR), not to accurately simulate the climate system response to that carbon release.

3. Results

3.1. Large Pockmarks and Fluid Conduits on the Chatham Rise

Numerous pockmarks of varying size are documented over >50,000 km^2 of the Chatham Rise, Canterbury Slope and Inner Bounty Trough, New Zealand (Figure 1). Multibeam data collected post 2010 greatly extend the distribution of seafloor depressions (pockmarks) documented in earlier surveys (Davy et al., 2010). Smaller pockmarks, 150–500 m wide and 3–8 m deep, occur at water depths between 500 and 700 m. Larger pockmarks, 1–7 km in diameter and 80–100 m deep, occur in 800- to 1,100-m water depths (Figure 1). There are numerous large, 1- to 5-km diameter (100 m deep) pockmarks on the southern margin of the plateau. There are also several giant pockmarks that are up to 12 km in diameter. At water depths of 1,500–2,400 m, across the inner-outer Bounty Trough boundary, there are pockmarks 1–5 km in diameter and 70–100 m deep (Figures 1 and S1).

Echosounder images from the northwestern part of the study area also identify numerous buried pockmarks formed on surfaces with high-amplitude reflections (Figure 3). With the recent development of high-resolution (better than 1-ms two-way traveltime and 1-m depth vertical) subbottom profilers that can penetrate up to 100 m in soft sediment, the pattern of glacial deposition becomes recognizable (Bull et al., 2006; Davy et al., 2010). Alternating banding in the seismic image (Figure 3) is attributed to glacial/interglacial cycles that affected the percentage of terrestrial input (80% carbonate during warm interstadial periods vs. <25% during glacials; Carter et al., 2000). We infer that the "darker" (high-amplitude reflections) horizons represent the higher-density terrestrial input during full glacials (red arrows in Figure 3b). Sedimentation rates in the region of this seismic section (Carter et al., 2000) are consistent with this interpretation (Davy et al., 2010) and provide the only plausible mechanism in agreement with the observed regional sedimentation cycles. Small pockmarks, approximately the size of the seafloor pockmarks (Figure 1), are also visible along these high-amplitude horizons. The pockmarks appear to have formed initially only at these horizons, which we interpret to mark glacial terminations (occurring every ~100,000 years). Pockmark morphology may persist in some instances until the next glacial termination, and we postulate these pockmarks have been a focus for repeated fluid venting at glacial terminations (Davy et al., 2010).

The origin of these pockmarks on the Chatham Rise and Bounty Trough has long been a mystery. Seafloor pockmarks have been attributed to sudden release of fluids or gas (Hovland et al., 2002; Hovland & Judd, 1988). And in an earlier study, it was hypothesized that the Chatham Rise pockmarks formed in response to destabilization of methane clathrates (Davy et al., 2010). The coincidence between the upper limit of shallow pockmarks and the top of methane gas hydrate stability in the ocean led to the hypothesis that pockmarks formed from methane gas hydrate dissociation at or near the glacial terminations following depressurization associated with sea-level lowering. However, a subsequent geochemical survey of porewater sulfate, methane, sulfide, and DIC profiles (section 3.2) found no evidence of methane.

An alternative mechanism proposed for the formation of small, shallow pockmarks along the western edge of the Canterbury Basin called upon groundwater flow through canyon walls induced by the Southland current (Hillman et al., 2015). However, it is difficult to explain the widespread occurrence of pockmarks across the Chatham Rise with this model, particularly in deeper waters.

A polygonal fault system appears beneath the pockmark fields in the 3-D seismic data that is indicative of significant dewatering (Cartwright & Lonergan, 1996; Hillman et al., 2015; Klaucke et al., 2018; Waghorn et al., 2018) It is conceivable therefore that water released from the compacting mudstones associated with the polygonal faulting could have facilitated some of the sea floor depressions. However, Hillman et al. (2015) could not establish any correlation between seafloor pockmarks and individual polygonal faults in data from the western Canterbury Basin.

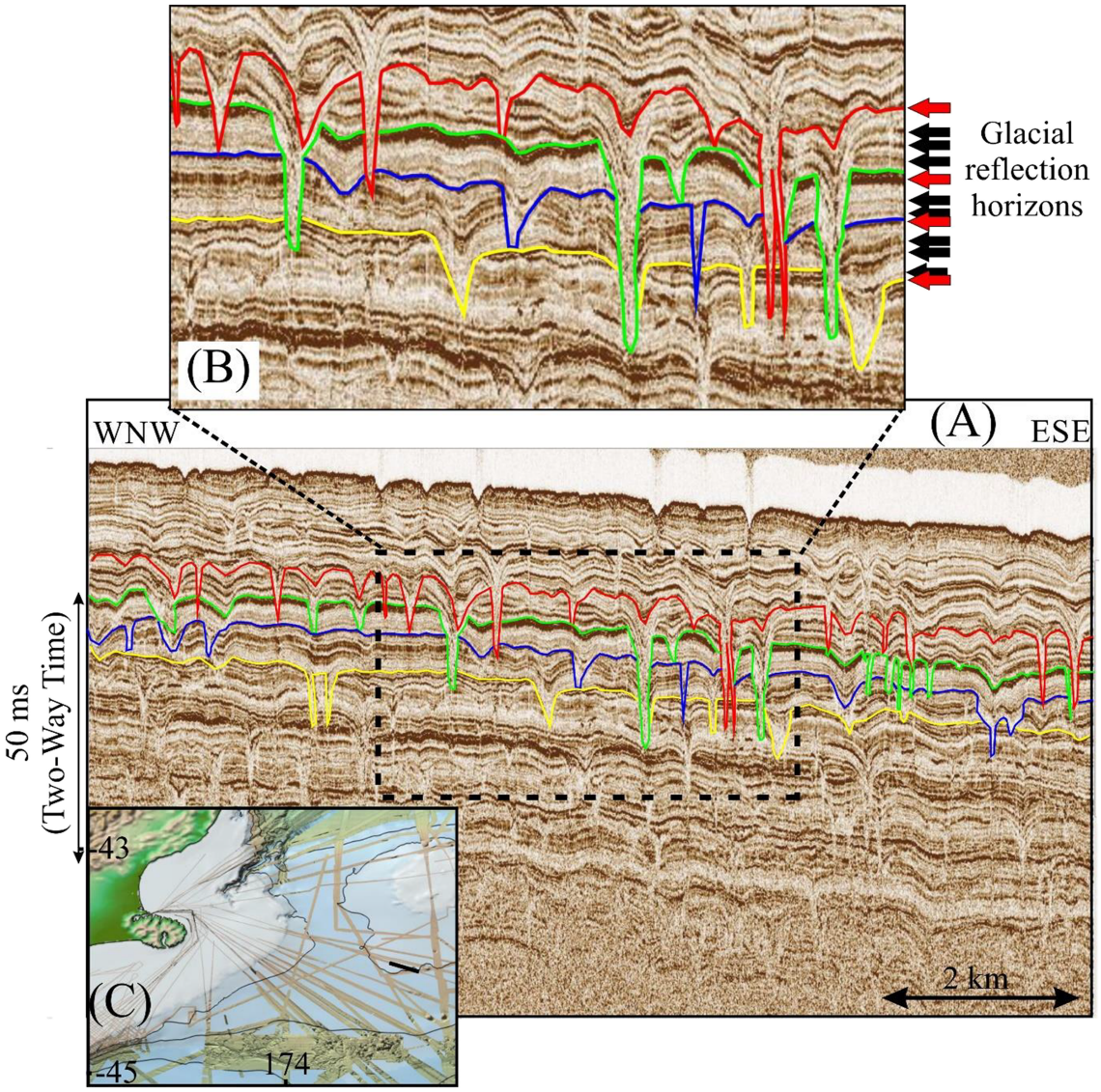

Figure 3. (A) A high-resolution sub-bottom PARASOUND profiler image of small pockmarks, 2-3 m deep and 100-200m wide, characteristic of pockmarks throughout the southwestern Chatham Rise area - in Zone 1 (Figure 1). Inset (B) highlights that the pockmarks are only occurring on top of every fourth stadial cycle (Red arrows). (C) Map of swath multibeam coverage with the black line highlighting the location of seismic profile (A). Parasound data is from R/V Sonne survey ANT26_3 (Gohl, 2003).

With widespread identification of Eocene-Miocene polygonal faulting in seismic data, Klaucke et al. (2018) suggested dewatering from opal A/CT transformation would cause the faults to act as fluid pipes. These authors proposed, that as fluids escaped from the faults at the seafloor, that scouring by bottom currents formed the seafloor depressions or pockmarks. The widespread presence of polygonal faulting observed over the Chatham Rise and within the Bounty Trough supports a compactional phase change and the release of water, whether from the opal-A/CT transition or the transition of calcareous ooze to chalk. However, this model does not account the large conduit structures we document beneath the pockmarks (Figure 4) nor the recurrence frequency of shallow pockmarks at glacial timescales (Davy et al., 2010). There is also no spatial correlation between shallow pockmarks and underlying polygonal faults. At the same time, these early Cenozoic fault networks may have facilitated the more recent release of fluids from near basement.

We present recently acquired geophysical evidence that the large pockmarks are associated with deeply rooted paths of fluid and gas migration. Seismic profiles above pockmarks on the Chatham Rise reveal numerous subsurface structures that are indicative of near-vertical gas and fluid migration (Figure 4). The

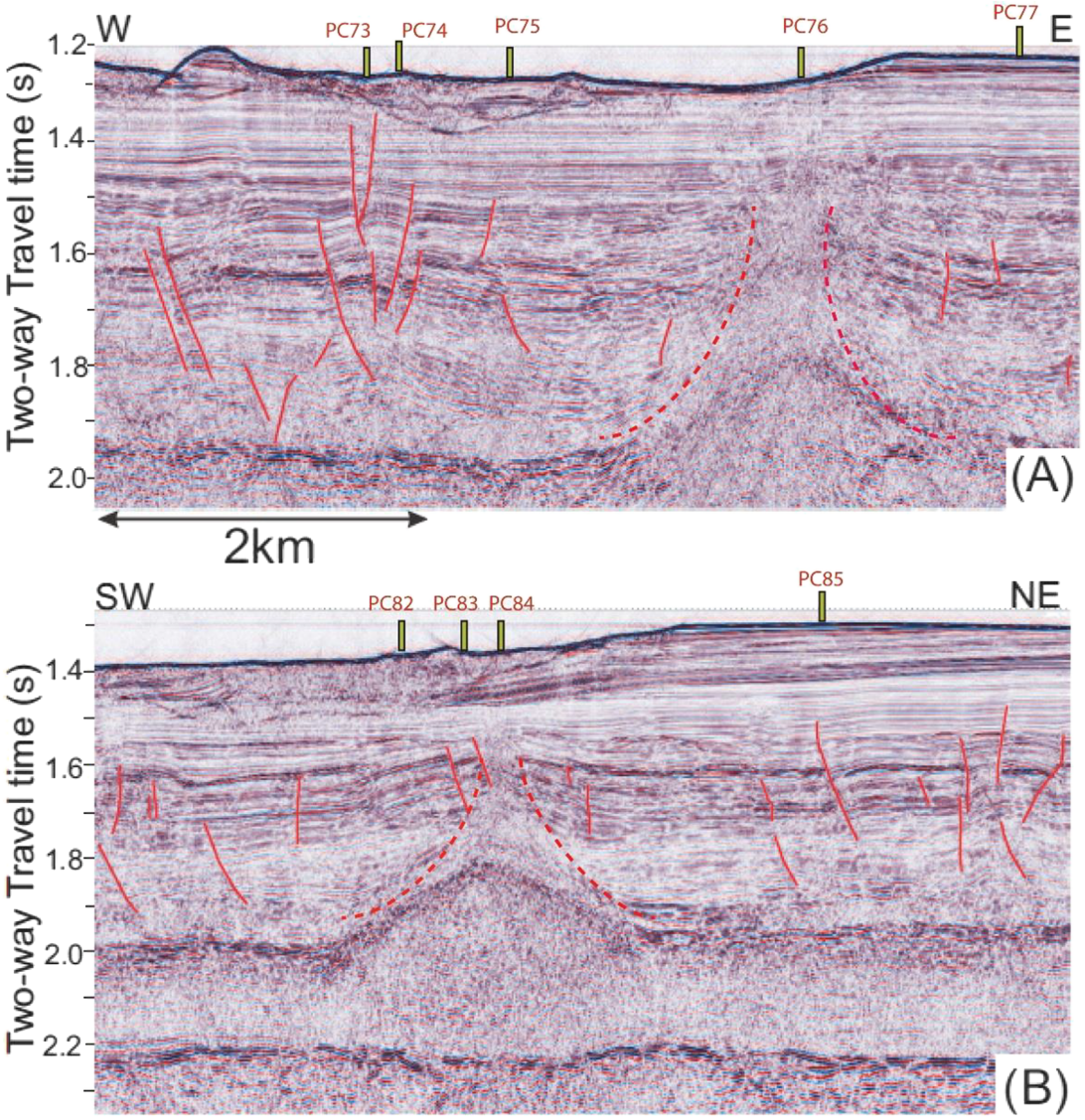

Figure 4. Seismic sections extending through piston core sites shown in Figure 1. The red dashed lines mark approximate boundaries of fluid-flow features ('vent conduits'). The solid red lines delineate the location of listric faults. Also shown are the location of piston cores (PC) collected during the 2013 expedition.

most prominent of these features is termed "vent conduits" because they lie directly beneath the large pockmarks (>1-km diameter) and provide a conspicuous pathway for fluid and gas migration to reach the seafloor. Elsewhere above, the subducted Hikurangi Plateau (Figure 4) upward fluid migration along faults is also evident. At the boundary between the inner and outer Bounty Trough, pockmarks occur above highly faulted crust, which in-turn, overlies the underlying eastern edge of the subducted Hikurangi Plateau (Figure 1; Davy, 2014). These faults would also act as pathways for upward fluid migration. In the seismic cross section (Figure 4a), listric faults and adjacent rotated sedimentary layers below Core PC73 (Figure 4a) are characteristic of an extensional depositional environment. Such faults are likely an expression of Eocene polygonal faulting that would have facilitated upward fluid migration (Waghorn et al., 2018). Further to the east, the sedimentary layers at 350–700 m below the seafloor are curved upward around a junction point more-or-less directly beneath the PC76 core (Figure 4). The conical-shaped features seen in the 2-D seismic sections (Figure 4) are characteristics of buoyancy-driven fluid and fluid-mobilized sediment flow (Waghorn et al., 2018). Subsurface vent conduits like those shown in Figure 2 are also observed beneath other large pockmarks across the southwest Chatham Rise.

Figure 5. a) PC75-1 benthic $\delta^{18}O$ stratigraphy; b) PC75-1 benthic $\delta^{13}C$ stratigraphy. There is no evidence of a negative $\delta^{13}C$ excursion during the last glacial termination as would be expected if the source of carbon responsible for the large $\Delta^{14}C$ excursions came from either mantle-derived CO_2 or from methane.

3.2. Geochemical Assessment of Modern and Past Methane Fluxes

To evaluate whether methane could be a primary source of gas beneath the pockmarks, the vertical methane flux and its spatial variation was investigated by analyzing sediment porewaters for anaerobic methane oxidation (Coffin et al., 2008; Coffin, Hamdan, et al., 2013; Coffin et al., 2014, 2015). The decline in sediment methane and porewater sulfate concentrations, associated with increased porewater DIC and sulfide, was used to identify a depth of the sulfate-methane-transition depth and used as a proxy for vertical methane migration. Sediment porosity and sulfate profiles provide an annual vertical methane flux. This analysis was conducted onboard to provide continuous comparison with the seismic data. The porewater data from Piston Cores PC75 and PC83 were taken during the 2013 SO226/2 expedition. Tables S2 and S3 and Figures S3 and S4 summarize the porewater sulfate (SO_4^{-2}), methane (CH_4), DIC, and the stable carbon isotope ($\delta^{13}C$) results for porewater profiles from these cores. The following observations confirm that there is no vertical migration of methane at these locations; 1) Low background CH_4 concentrations, near the limits of detection at all locations; (2) the vertical profiles show deep CH_4 concentrations declining, while DIC increases proportionally with SO_4^{-2}. In this study there was no relation between SO_4^{-2} and CH_4. SO_4^{-2} was uncharacteristically high throughout the cores. In an active CH_4 flux region, SO_4^{-2} typically disappears from porewater in the top 100 cm (Coffin, 2008). Anaerobic oxidation of CH_4 in porewaters produces an increase in DIC concentration, and the $\delta^{13}C$ of DIC becomes strongly depleted. No such geochemical trend was observed, and the moderate $\delta^{13}C$ DIC change suggests that there has been shallow organoclastic sediment carbon cycling but no methane oxidation.

We cannot exclude the possibility that methane has, in the past, contributed to the flux of fluids from the subsurface structural features. But over the course of the past 25 kyr (the length of our core records), the benthic $\delta^{13}C$ stratigraphy from available piston cores does not contain any anomalously low values. In fact, the PC75 benthic $\delta^{13}C$ stratigraphy documents a positive excursion during the deglaciation when the $\Delta^{14}C$ values exhibit a negative excursion (Figure 5). Sikes et al. (2017) found a similar positive $\delta^{13}C$ excursion in another core (79JPC) taken at similar water depth from the Bay of Plenty.

3.3. Evidence of ^{14}C-Depleted Fluids Entering the Ocean From Subsurface Reservoirs Beneath Chatham Rise at the Glacial Termination

The uppermost sediments at the PC75 core site are undisturbed. The planktic and benthic $\delta^{18}O$ stratigraphies from this core document continuous sediment accumulation since the LGM (Figure 5). The radiocarbon ages

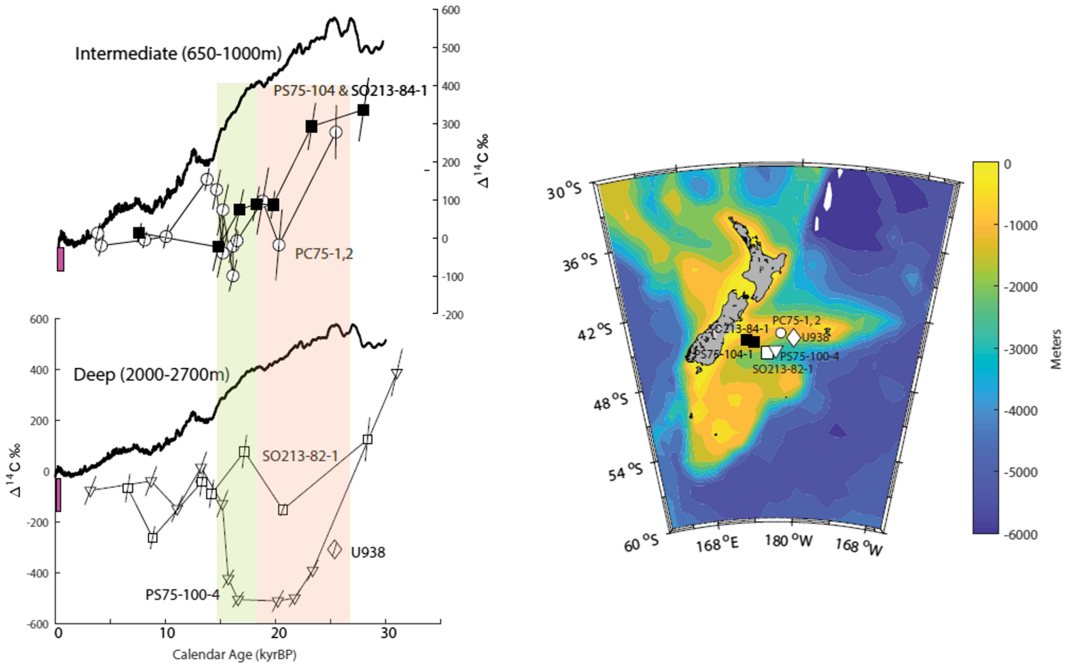

Figure 6. Left panel, $\Delta^{14}C$ for the atmosphere (INTCAL13, black solid lines), shallow (upper panel) and deep (lower panel) water cores from the Chatham Rise and Bounty Trough (Right Panel). Error bars are the combined uncertainties of the calendar age model and $\Delta^{14}C$. The offset between the modern atmosphere and the modern ocean are indicated by the vertical red bars. The panel shading indicates the late glacial (red) and early deglacial (yellow).

obtained for both planktic and benthic foraminifera from this core were converted to radiocarbon activity ($\Delta^{14}C$; Figure 6).

Today, the PC75 core location is bathed by well-ventilated, relatively "young" Antarctic Intermediate Water. The $\Delta^{14}C$ offset between Antarctic Intermediate Water and the atmosphere today is ~100–150‰. During the late glacial and in the early deglacial however, the benthic-atmospheric $\Delta^{14}C$ offset ($\Delta\Delta^{14}C$) at the PC75 site increased to ~400‰ (Figure 6). Ronge et al.'s PS75-104 and SO213-84-1 record documents similar values (Figure 6) to those of PC75. At deeper water depths, between 2,000 and 2,500 m, the $\Delta\Delta^{14}C$ offset between Pacific Deep Water and the atmosphere today is ~200‰, reflecting the fact that Pacific Deep Water is older and has acquired respired carbon along its path from the North Pacific to the Southern Ocean. In the sediment cores from the Bounty Trough analyzed by Ronge et al. (2016), the benthic-atmosphere $\Delta\Delta^{14}C$ values during the late glacial and early deglacial increased to ~1,000‰ (Figure 5). Sikes et al. (2000) also found similarly ^{14}C-depleted values in association with Kawakawa tephra in a core not far from Ronge et al.'s core in the Bounty Trough (Figure 6). Each of these cores is located close to large pockmarks that occur within the Bounty Trough (Figure 1). It appears from these records that highly ^{14}C-depleted values were recorded across a wide range of water depths and across the Chatham Rise and Bounty Trough beginning at approximately 25 kyr BP, in close temporal association with the Kawakawa tephra. But similarly depleted values are not observed in the intermediate depth cores from the Bay of Plenty to the north of the Chatham Rise (Rose et al., 2010; Sikes et al., 2016).

4. Discussion

4.1. Timing of Last Episode of Pockmark Formation

A central tenant of our hypothesis is that pockmarks formed at glacial terminations. Here we consider glacial terminations to represent the time period spanning when the Earth's climate reached a minimum temperature (often referred to as Glacial Maxima) and the onset of warming that accompanied the actual deglaciation. In this context, the last glacial termination spans the interval of time between about 30 and ~16 kyr BP. This is an important distinction because there were many events centered on this time period that cannot be simply classified as either the LGM or the deglaciation. Evidence presented in this study illustrates that $\Delta^{14}C$ began to decrease at sites on the Chatham Rise and Bounty Trough near 25 kyr BP (Figure 6). The

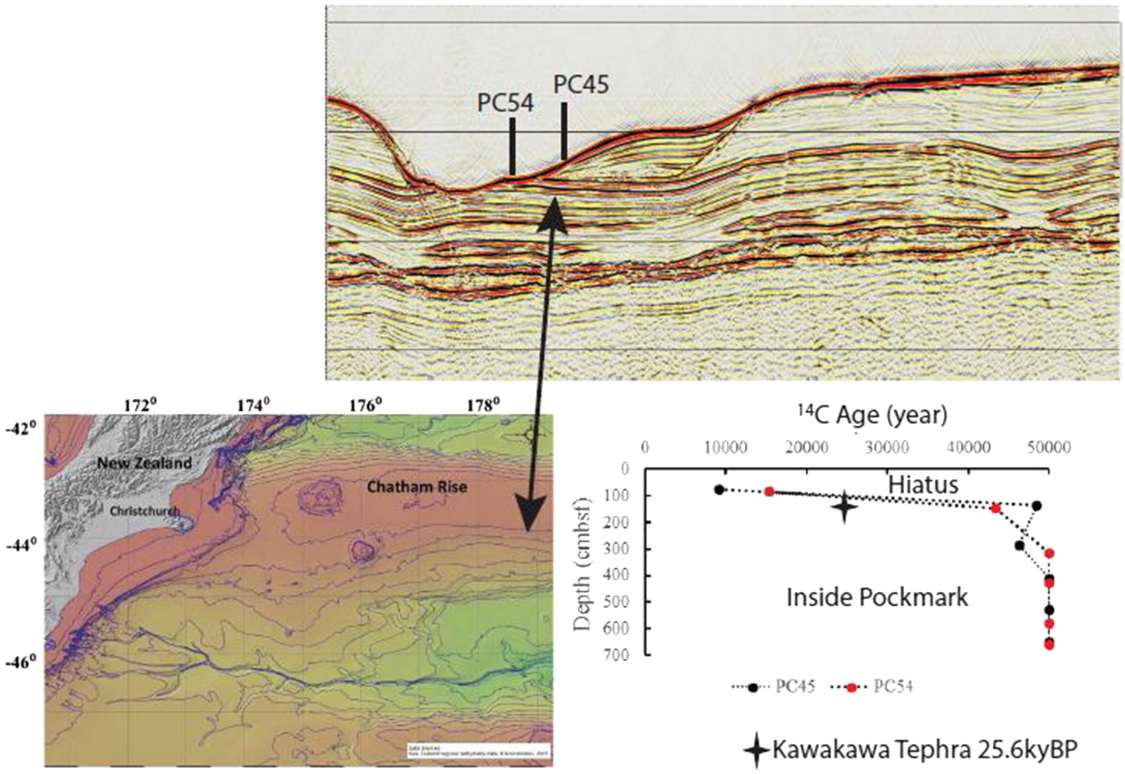

Figure 7. ^{14}C ages of bulk sediment (lower right panel) from two cores collected from a pockmark (upper right panel) on the Chatham Rise. Note the dramatic increase in age just below the Kawakawa tephra in PC45, marking a hiatus of missing sediment that was lost when the pockmark formed just prior to the deposition of the tephra at 25.6kyBP.

well-dated Kawakawa tephra was also deposited at 25.6 kyr BP (Lowe et al., 2013; Sikes & Guilderson, 2016). Atmospheric $\Delta^{14}C$ also began to decrease at this time (Figure 6). In another study, Stott et al. (2019) found that radiocarbon activity values at intermediate depths in the eastern equatorial Pacific also began to decrease at about 25 kyr BP as they did at a deep water site in the South Atlantic (Skinner et al., 2010).

The precise timing of each pockmark exposed at the surface today cannot be ascertained with the data we currently have. However, there are several lines of evidence that indicate the most recent phase of pockmark formation occurred during the last glacial termination. This includes the contrasting ^{14}C and $\delta^{18}O$ stratigraphies from biogenic carbonates deposited within pockmarks (above the base of a pockmark horizon) compared to the isotope stratigraphies from cores collected outside of, but adjacent to, pockmarks. To illustrate this, we selected two cores collected from within one of the pockmarks (Figure 7). The ^{14}C age stratigraphy of the bulk inorganic carbon is shown in Cores PC45 and PC54. Both cores exhibit a dramatic increase in age below 136 cm. The PC45 core contains the Kawakawa tephra at 135 cm (Figure 7). The ^{14}C ages at 136 cm, immediately below the tephra, are radiocarbon dead, implying that there is a hiatus of missing sediment just below the 25.6 kyr BP tephra horizon. The first sediments to be deposited within the pockmark coincide with the tephra itself, and therefore, it appears that this pockmark formed at the time of the Kawakawa Tephra, 25.6 kyr BP. There is an ongoing effort to conduct similar dating of sediments within the most recent pockmarks to verify the timing of sediments that first filled the pockmarks after they formed.

4.2. Source of ^{14}C-Depleted Carbon

We have shown that the biogenic sediments that were deposited adjacent to the larger pockmarks on the Chatham Rise and Bounty Trough document large negative $\Delta\Delta^{14}C$ anomalies during the last glacial termination beginning at ~25 kyr BP that are not observed at other sites near the Chatham Rise. And while it will be important to determine the extent of these radiocarbon anomalies at various depths and at other sites

across the Chatham Rise, Rose et al. (2010) and Sikes et al. (2016) found no large $\Delta\Delta^{14}C$ excursion at shallow intermediate water depths in the Bay of Plenty. We take this initial set of observations to indicate the excursions were restricted to sites on the Chatham Rise and Bounty Trough where there are large pockmarks above the subsurface conduits. We also find that there is no $\delta^{13}C$-depleted biogenic carbonate accompanying the $\Delta^{14}C$ excursions that would be indicative of methane or petroleum carbon oxidation. When these isotope data are combined with the seismic data, it is clear that overpressurized fluids released from subsurface reservoirs would be the most plausible source of carbon with these geochemical characteristics. If "old" respired carbon from a formally isolated water mass had been responsible for the depleted $\Delta^{14}C$ values observed in the benthic records, those waters would have also carried a distinctly depleted $\delta^{13}C$ DIC signature, which is not observed (Figure 5). Similarly, if the source of carbon responsible for the depleted $\Delta^{14}C$ values had come from release of methane-rich fluids, that too would have carried a distinctly depleted $\delta^{13}C$ value, which is not observed in the biogenic records. The porewater geochemical profiles at 20 other locations across the study region are all consistent with that of PC75 and PC83 (Coffin, Rose, et al., 2013). The extremely low rates of methane flux inferred from the sulfate profiles at all core sites and the lack of any negative $\delta^{13}C$ excursions observed in the biogenic carbonates deposited during the most recent phase of pockmark formation are not consistent with a methane gas source.

Based on the large negative $\Delta^{14}C$ anomaly and lack of a negative $\delta^{13}C$ excursion at the last glacial termination, the most plausible source of carbon would be CO_2 from dissociated limestones at depth beneath the Rise. This is the same carbon source that forms liquid CO_2 that vents today in the western Pacific on Mariana hydrothermal vent system (Lupton et al., 2006). But on the Chatham Rise and Bounty Trough, there are no hydrothermal vents. Dissociated carbonates from the subducted Hikurangi Plateau would form buoyant CO_2 that would migrate upward though the fault systems towards the surface.

The depth of the underlying flat-subducted Hikurangi beneath the Chatham Rise and Bounty Trough is largely unknown but is expected to be somewhere between 8 and 20 km. With an average temperature gradient of 40 °C/km, this implies a temperature between 320 and 800 °C for the top of the underlying plateau. Dissociation of carbonate is a balance between CO_2 concentration and temperature (Stanmore & Gilot, 2005). At lower temperatures, the rate of dissociation is lower and depends on the rate removal of existing CO_2 along faults. Importantly, there has been a massive amount of limestone subducted beneath the Chatham Rise and Bounty Trough for 100×10^6 years. The dissociation rate may be small, but the time for accumulation of dissociated CO_2 is large. There has also been an ongoing history of volcanism along the Chatham Rise since the Cretaceous (Wood & Herzer, 1993). Increased temperatures associated with volcanism will have enhanced CO_2 release. It may also facilitate release of stored CO_2 at depth. Notably, the large volcanic Kawakawa tephra was deposited across the Chatham Rise 25.6 kyr BP (Lowe et al., 2013; Sikes & Guilderson, 2016) just as the large $\Delta^{14}C$ excursion began (Figure 6).

The very large negative $\Delta^{14}C$ excursion documented by Ronge et al. (2016) from sediments cores taken at the deeper water depths within the Bounty Trough is also adjacent to one of the giant pockmarks (Figure 5). Ronge et al. originally called upon transport of ^{14}C-dead carbon from hydrothermal systems located on the EPR to explain the excursion seen in their Bounty Trough cores. Using a 1-D box model and upscaling, Ronge et al. (2016) estimated that a ^{14}C-dead CO_2 flux of 0.16 GtC/year is required to decrease the entire Southwest Pacific (40–60°S, 110–180°W) $\Delta\Delta^{14}C$ by ~500‰, as observed in their PS75/059-2 record on the EPR and PS75/100-2 on Chatham Rise. However, given the long duration of the $\Delta^{14}C$ excursion, it seems likely that ocean mixing would have diluted such a signal by the time it reached the Chatham Rise. This mixing process is missing in Ronge et al.'s approach. To take this effect into account and to evaluate the impact of ^{14}C-dead DIC flux from the EPR at Chatham Rise, we conducted independent experiments using an Earth System Model of intermediate complexity (cGENIE; section 2). Although cGENIE is a relatively low-resolution model, it is a suitable tool to evaluate basin-scale radiocarbon budgets over timescales of several thousand years. In these experiments, a range of ^{14}C-dead DIC between 0.16 and 1.28 GtC/year was released directly into a 10° by 11°, ~570-m-thick (3,008–3,575 m) grid box overlying the EPR, where Ronge et al.'s PS75/059-2 core is located. Deep ocean stratification is enhanced in these simulations through brine rejection in the Southern Ocean (see section 2). This is a relatively crude approach, but we are not intending to match all the observations that constrain the "LGM" state. Rather, the focus here is how the radiocarbon field in the SW pacific responds to ^{14}C-Dead DIC input from the EPR under a stronger stratification state.

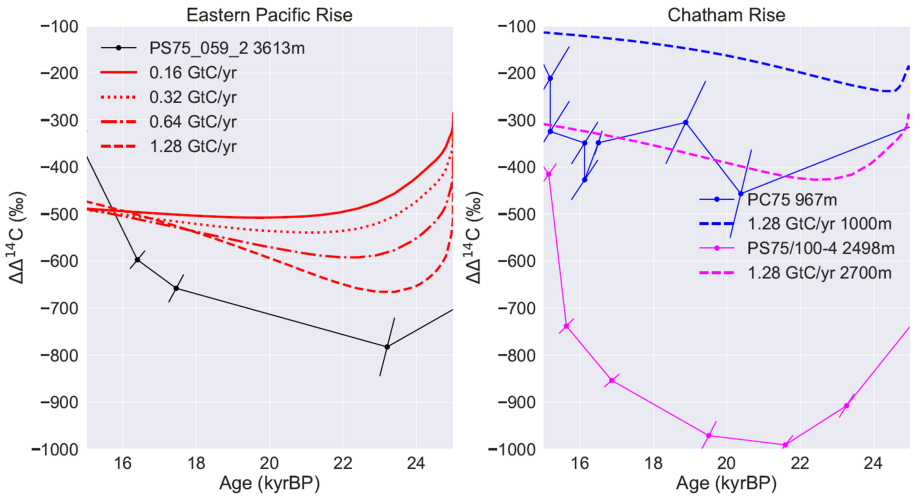

Figure 8. Left panel, red lines represent simulated Δ14C difference between the grid box where ^{14}C-dead DIC was injected and atmosphere ($\Delta\Delta^{14}$C) at different injection rates; the black solid line denotes the PS75-059-2 record (Ronge et al., 2016; Ronge et al., 2019) Right panel, simulated $\Delta\Delta^{14}$C response at ~1000m (the blue dash line) and ~2700m (the purple dash line) on Chatham Rise (CR) under the most extreme DIC injection rate scenario (1.28 GtC/yr); the blue and purple solid line represent the PC75 (this study) and PS75/100-4 (Ronge et al., 2016) record, respectively.

For an injection rate of 0.16 GtC/year as called for by Ronge et al., the magnitude of the simulated $\Delta\Delta^{14}$C excursion in the injected grid box on EPR only reaches 250‰ (Figure 4, blue), not 500‰ as simulated by their 1-box model. The observed ~400‰ decrease in $\Delta\Delta^{14}$C on EPR is achieved only in a simulation with an injection rate of 1.28 GtC/year (Figure 8, left panel, the red curve). However, even in this extreme injection scenario, the simulated $\Delta\Delta^{14}$C change on Chatham Rise at 2,700 m (close to Ronge's PS75/100-2) is no larger than 150‰ (Figure 8, right panel), far smaller than is observed in the reconstructed Δ^{14}C records (Figure 6). And importantly, this small transient reduction in $\Delta\Delta^{14}$C is not the result of anomalously old ^{14}C from the EPR. Rather, it is caused by the reduced ventilation invoked in the model experiment by enhancing deep water stratification. Furthermore, there is no negative Δ^{14}C excursion simulated at the PC75 core location (~1,000 m) on Chatham Rise. These model results do not support the suggestion that ^{14}C -dead DIC can be transported from hydrothermal systems as far away as the EPR to produce the large excursions observed on the Chatham Rise. It is also important to emphasize that mantle-derived CO_2 carries a ^{13}C-depleted signature of approximately −5‰ to −7‰ (Deines, 2002). There is no negative excursion in benthic δ^{13}C in association with the Δ^{14}C excursions on Chatham Rise (Figure 3). Together, the model and observational results presented here make clear that a release of ^{14}C-dead carbon at any single point in the ocean on the EPR or elsewhere will be diluted within a relatively short distance. This means that the large Δ^{14}C anomalies observed on the Chatham Rise must have come from local sources. The subsurface conduits beneath the pockmarks represent the path those carbon-rich fluids would have taken to the surface. Dissociated Mesozoic carbonate at depth is the most plausible source of that carbon because it would provide ^{14}C-dead carbon and leave no δ^{13}C anomaly consistent with the data. One of the open questions that remains is whether there was carbonate dissolution upon release of the carbon-rich fluids to the overlying ocean. The most obvious place to look for evidence of dissolution would be at sites close to the Ronge et al cores where the Δ^{14}C anomalies are large.

4.3. Potential Valving Mechanism for CO_2 Storage and Release

The specific "valving mechanism" for CO_2 accumulation and release, and the formation mechanism for pockmarks at the surface, remains a mystery. The seismic observations imply that the valving mechanism must regulate storage and release of CO_2-rich fluids beneath the sea floor on a regular recurring frequency. With this in mind, several observations point to a link between temperature, sea level, and CO_2 hydrate stability that accompanies glacial terminations. The first observation is that the shallowest depth where

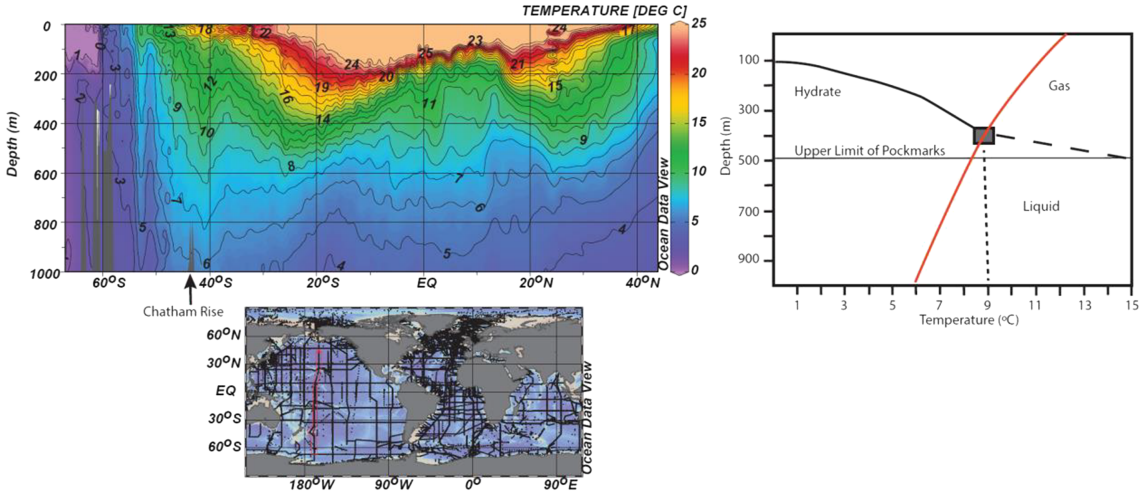

Figure 9. Ocean temperature within the upper 1000m in the Pacific (GLODAP v2) and the three-phase stability of pure CO_2 in seawater. The red line in the right panel is the present day temperature over the Chatham Rise at 44°S.

pockmarks occur on the Chatham Rise (Region 1) is at 500 m. In the modern ocean, the waters at 44°S and 500 m over the Chatham Rise are ~7 °C and thus, ~2 °C below the hydrate stability temperature (Figure 9). Depressurization from sea level change at constant temperature would move the upper limit of pockmark formation near the phase boundary between hydrate and free gas.

There are strong lateral and vertical temperature gradients in these water depths on the Chatham Rise (Figure 9). While sea level changes at temperatures above ~9 °C would have little influence on this phase transition, hydrate stability would be very sensitive to temperature changes. With these factors in mind, there remains many open questions about what may influence hydrate stability. There is a critical need to obtain additional well-resolved records of $\delta^{18}O$ during the last glacial termination from which to develop a better spatial and temporal depiction of when temperatures varied across the Chatham Rise and Bounty Trough. Furthermore, the high solubility of CO_2 requires considerably higher concentrations of CO_2 for formation of CO_2 hydrate than methane for methane hydrate. More accurate knowledge of gas composition is also needed since the addition of small amounts of other gases significantly alters the CO_2-hydrate phase boundary. This information will allow modeling of the predicted movement of top and base of hydrate stability within the sediments through time, specifically accounting for the propagation of temperature signals into the seafloor and the possible thermal sink due to the endothermic nature of hydrate dissociation (Goto et al., 2016). Predicted hydrate dissociation could then be compared to timing of pockmark formation and release of old CO_2 reflected in $\Delta^{14}C$ records.

CO_2 hydrate may have two important roles. It could constitute a near-seafloor ephemeral capacitor, temporally storing CO_2. It may also act as seal inhibiting fluid flow, leading to pressure buildup of CO_2-rich fluids followed by sudden release when the seal dissociates. Ephemeral capacitors unrelated to hydrate could also be present deeper in the sediments: CO_2 could be released from pore waters during depressurization leading to an increase of CO_2 flux toward the seafloor. The role of supercritical CO_2 deeper in the seafloor and variations of its phase boundary following pressure or temperature changes and leading to CO_2 release of uptake will also need to be investigated. From a near-seafloor perspective, these mechanisms would constitute a variation of the source strength for CO_2 flux through glacial cycles, rather than near seafloor storage capacity of CO_2 in the form of hydrate or a temporary seal that dissociates at the end of glacial maxima. These questions motivate our ongoing research.

Whatever the valving mechanism is, it seems evident from the recurrence frequency of pockmarks seen in the seismic sections that CO_2 accumulated over a glaciation and was released rapidly at/near glacial terminations. In this sense the Chatham Rise and Bounty Trough act as a capacitor for CO_2, analogous to an electrical capacitor that regulates the flux of electrons within a circuit. This intriguing question of what regulates

the flow of CO_2 from beneath the Chatham Rise remains an open question and an important topic of ongoing research. Nonetheless, we emphasize that whatever the specific mechanism is that modulates the flux of gas, it is clear that pockmark formation on the Chatham Rise and Bounty Trough has been associated with rapid release of gas and fluids at/near glacial terminations.

The available data cannot be used to estimate how much carbon was released at the last glacial termination from sites on the Chatham Rise. But the magnitude and duration of the $\Delta^{14}C$ excursions imply a sustained release of carbon over several thousand years. If these $\Delta^{14}C$ excursions are seen only at a small number of sites on the Rise, these may not be a significant source of carbon to the ocean at the glacial termination. On the other hand, because of the large number of pockmarks across the Chatham Rise and Bounty Trough (Figure S1), it is reasonable to consider that carbon released from numerous pockmarks on Chatham Rise could have influenced the ocean's carbon budget at the last glacial termination. In this case the release of old carbon may have contributed to the increased reservoir ages of intermediate and surface waters in the southwest Pacific (Rose et al., 2010; Shao et al., 2019; Sikes & Guilderson, 2016; Skinner et al., 2015). Further studies will now be necessary to evaluate whether there were changes in regional carbonate chemistry close to and away from the sites of carbon release.

5. Conclusions

It is increasingly evident that there were several factors influencing the carbon budget of the ocean and the atmosphere simultaneously at the last glacial termination. These likely included some change in the residence time of carbon within the ocean together with geologic processes that include hydrothermal venting (Broecker et al., 2015; Huybers & Langmuir, 2017; Lund et al., 2016; Stott et al., 2019; Stott & Timmermann, 2011) and release of carbon from subsurface reservoirs such as those beneath Chatham Rise. What is not yet clear, however, is how various processes acted in concert with high latitude ocean/atmospheric dynamics to synchronize the glacial cycles of pCO_2 with the orbital variations. Stott and Timmermann (2011) argued that one part of this synchronization may involve temperature changes that are propagated from the Southern Ocean to sites where CO_2 accumulates during glaciations and can be destabilized at glacial terminations. Other studies have argued that a trigger mechanism for release of geologic carbon from hydrothermal systems involves mantle decompression and subsequent invigoration of mantle convection that can promote volcanism (Broecker et al., 2015; Huybers & Langmuir, 2017; Lund & Asimow, 2011). In the case of Chatham Rise, the mechanism responsible for release of carbon-rich fluids responsible for the pockmarks and the $\Delta^{14}C$ anomalies near the deglaciation is yet unknown, but our results indicate it involved buoyancy-driven fluid escape. An ultimate test of our hypothesis awaits deep coring into previous glacial terminations to date the timing of previous pockmark formation. But based solely on the recurrence of pockmarks seen in the seismic records, we would conclude that the Chatham Rise must act as a carbon capacitor, charging with CO_2-rich fluids from a subsurface carbon reservoir during glaciations and then releasing the stored carbon to the overlying ocean.

Acknowledgments
During this study, friend and close colleague Robert Thunell passed. This paper is dedicated to his memory and the important influence he had on the field. We thank two anonymous reviewers for their thoughtful and helpful evaluations of this work. The authors also express gratitude to Patrick Rafter for helpful discussion and suggestions. L. S. and J. S. were supported by an NSF Grant (MG&G 1558990). Funding for B. D., H. N., and I. P. was provided by the Royal Society of New Zealand "Marsden" Fund, Grant UOA1022. R. C. and P. R. were supported by funds from Department of Energy, National Energy Technology Laboratory Morgantown West Virginia, USA. The R/V SONNE cruise SO-226, led by GEOMAR Helmholtz Centre of Ocean Sciences Kiel, was funded by Federal Ministry of Education and Research, Germany through Grant 03G0226A. We thank captains Lutz Mallon and Oliver Meyer with their entire crew for their excellent support. The pore water geochemical data and bulk sediment radiocarbon ages presented in this paper are archived in the PANGAEA data repository (https://doi.pangaea.de/10.1594/PANGAEA.906048). The benthic foraminiferal radiocarbon data for Piston Core PC75 are archived online (https://doi.org/10.1594/PANGAEA.901237). Multibeam data are archived online (https://www.marine-geo.org/tools and https://data.gns.cri.nz/pbe/. The Parasound seismic reflection data (Figure 3) and the seismic reflection lines for Figures 4a, 4b, 7, and S2.4 and all in SEGY format and two GMT-format grids of bathymetry in Figures 1 and 2 are freely available online (https://shop.gns.cri.nz/Chatham_Rise_Bounty_Trough_data at DOI: 10.21420/DMFH-5593).

References

Adkins, J. F. (2013). The role of deep ocean circulation in setting glacial climates. *Paleoceanography*, *28*(3), 539–561. https://doi.org/10.1002/palo.20046

Adkins, J. F., McIntyre, K., & Schrag, D. P. (2002). The salinity, temperature, and $\delta^{18}O$ of the glacial deep ocean. *Science*, *298*(5599), 1769–1773. https://doi.org/10.1126/science.1076252

Adkins, J. F., & Schrag, D. P. (2003). Reconstructing Last Glacial Maximum bottom water salinities from deep-sea sediment pore fluid profiles. *Earth and Planetary Science Letters*, *216*(1-2), 109–123.

Anderson, R. F., Ali, S., Bradtmiller, L. I., Nielsen, S. H. H., Fleisher, M. Q., Anderson, B. E., & Burckle, L. H. (2009). Wind-driven upwelling in the Southern Ocean and the deglacial rise in atmospheric CO_2. *Science*, *323*(5920), 1443–1448. https://doi.org/10.1126/science.1167441

Andreassen, K., Hubbard, A., Winsborrow, M., Patton, H., Vadakkepuliyambatta, S., Plaza-Faverola, A., et al. (2017). Massive blow-out craters formed by hydrate-controlled methane expulsion from the Arctic seafloor. *Science*, *356*(6341), 948–953. https://doi.org/10.1126/science.aal4500

Basak, C., Fröllje, H., Lamy, F., Gersonde, R., Benz, V., Anderson, R. F., et al. (2018). Breakup of last glacial deep stratification in the South Pacific. *Science*, *359*(6378), 900–904. https://doi.org/10.1126/science.aao2473

Böttner, C., Berndt, C., Reinardy, B. T. I., Geersen, J., Karstens, J., Bull, J. M., et al. (2019). Pockmarks in the Witch Ground Basin, Central North Sea. *Geochemistry, Geophysics, Geosystems*, *20*, 1698–1719. https://doi.org/10.1029/2018gc008068

Broecker, W., Barker, S., Clark, E., Hajdas, I., Bonani, G., & Stott, L. (2004). Ventilation of the glacial deep Pacific Ocean. *Science*, *306*(5699), 1169–1172. https://doi.org/10.1126/science.1102293

Broecker, W., Clark, E., & Barker, S. (2008). Near constancy of the Pacific Ocean surface to mid-depth radiocarbon-age difference over the last 20 kyr. *Earth and Planetary Science Letters*, *274*(3–4), 322–326. https://doi.org/10.1016/j.epsl.2008.07.035

Broecker, W. S., Yu, J., & Putnam, A. E. (2015). Two contributors to the glacial CO_2 decline. *Earth and Planetary Science Letters*, *429*, 191–196. https://doi.org/10.1016/j.epsl.2015.07.019

Bryan, S. P., Marchitto, T. M., & Lehman, S. J. (2010). The release of ^{14}C-depleted carbon from the deep ocean during the last deglaciation: Evidence from the Arabian Sea. *Earth and Planetary Science Letters*, *298*(1-2), 244–254. https://doi.org/10.1016/j.epsl.2010.08.025

Bull, J. M., Barnes, P. M., Lamarche, G., Sanderson, D. J., Cowie, P. A., Taylor, S. K., & Dix, J. K. (2006). High-resolution record of displacement accumulation on an active normal fault: Implications for models of slip accumulation during repeated earthquakes. *Journal of Structural Geology*, *28*(7), 1146–1166. https://doi.org/10.1016/j.jsg.2006.03.006

Burke, A., & Robinson, L. F. (2012). The Southern Ocean's role in carbon exchange during the last deglaciation. *Science*, *335*(6068), 557–561. https://doi.org/10.1126/science.1208163

Cao, L., Eby, M., Ridgwell, A., Caldeira, K., Archer, D., Ishida, A., et al. (2009). The role of ocean transport in the uptake of anthropogenic CO_2. *Biogeosciences*, *6*(3), 375–390. https://doi.org/10.5194/bg-6-375-2009

Carter, L., Neil, H. L., & McCave, I. N. (2000). Glacial to interglacial changes in non-carbonate and carbonate accumulation in the SW Pacific Ocean, New Zealand. *Palaeogeography, Palaeoclimatology, Palaeoecology*, *162*(3), 333–356. https://doi.org/10.1016/S0031-0182(00)00137-1

Cartwright, J. A., & Lonergan, L. (1996). Volumetric contraction during the compaction of mudrocks: A mechanism for the development of regional-scale polygonal fault systems. *Basin Research*, *8*(2), 183–193. https://doi.org/10.1046/j.1365-2117.1996.01536.x

Coffin, R., Hamdan, L., Plummer, R., Smith, J., Gardner, J., Hagen, R., & Wood, W. (2008). Analysis of methane and sulfate flux in methane-charged sediments from the Mississippi Canyon, Gulf of Mexico. *Marine and Petroleum Geology*, *25*(9), 977–987. https://doi.org/10.1016/j.marpetgeo.2008.01.014

Coffin, R. B., Hamdan, L., Smith, J. P., Plummer, R., Millholland, L., & Larson, R. (2013). Spatial variation in shallow sediment methane source and cycling along the Alaskan Beaufort Sea. *Marine and Petroleum Geology*. https://doi.org/10.1016/j.marpetgeo.2013.05.002

Coffin, R. B., Hamdan, L. J., Smith, J. P., Rose, P. S., Plummer, R. E., Yoza, B., et al. (2014). Contribution of vertical methane flux to shallow sediment carbon pools across Porangahau Ridge, New Zealand. *Energies*, *7*, 5332–5356. https://doi.org/10.3390/en7085332

Coffin, R. B., Osburn, C. L., Plummer, R. E., Smith, J. P., Rose, P. S., & Grabowski, K. S. (2015). Deep sediment-sourced methane contribution to shallow sediment organic carbon: Atwater Valley, Texas-Louisiana Shelf, Gulf of Mexico. *Energies*, *8*(3), 1561–1583. https://doi.org/10.3390/en8031561

Coffin, R. B., Rose, P. R., Yosa, B., & Millholland, L. (2013). Geochemical evaluation of climate change on the Chatham Rise. US Naval Research Laboratory, Technical Memorandum.

Davy, B. (2014). Rotation and offset of the Gondwana convergent margin in the New Zealand region following Cretaceous jamming of Hikurangi Plateau large igneous province subduction. *Tectonics*, *33*, 1577–1595. https://doi.org/10.1002/2014TC003629

Davy, B., Pecher, I., Wood, R., Carter, L., & Gohl, K. (2010). Gas escape features off New Zealand: Evidence of massive release of methane from hydrates. *Geophysical Research Letters*, *37*, L21309. https://doi.org/10.1029/2010GL045184

Deines, P. (2002). The carbon isotope geochemistry of mantle xenoliths. *Earth-Science Reviews*, *58*(3), 247–278. https://doi.org/10.1016/S0012-8252(02)00064-8

de Mahiques, M. M., Schattner, U., Lazar, M., Sumida, P. Y. G., & Souza, L. A. P. (2017). An extensive pockmark field on the upper Atlantic margin of Southeast Brazil: Spatial analysis and its relationship with salt diapirism. *Heliyon*, *3*(2), e00257. https://doi.org/10.1016/j.heliyon.2017.e00257

Dickens, G. R., Koelling, M., Smith, D. C., Schieders, L., & Scientists, O. E. (2007). Rhizon sampling of pore waters on scientific drilling expeditions: An example from the IODP Expeditions 302, Arctic Coring Expedtion (ACEX). *Scientific Drilling*, *4*, 22–25. https://doi.org/10.2204/iodp.sd.4.08.2007

Donahue, D. J., Linick, T. W., & Jull, A. J. T. (1990). Isotope-ration and background corrections for accelerator mass spectrometry radiocarbon measurements. *Radiocarbon*, *32*(2), 135–142.

Edwards, N. R., & Marsh, R. (2005). Uncertainties due to transport-parameter sensitivity in an efficient 3-D ocean-climate model. *Climate Dynamics*, *24*(4), 415–433. https://doi.org/10.1007/s00382-004-0508-8

Feldens, P., Schmidt, M., Mücke, I., Augustin, N., Al-Farawati, R., Orif, M., & Faber, E. (2016). Expelled subsalt fluids form a pockmark field in the eastern Red Sea. *Geo-Marine Letters*, *36*(5), 339–352. https://doi.org/10.1007/s00367-016-0451-9

Gohl, K. (2003), Structure and dynamics of a submarine continent: Tectonic-magmatic evolution of the Campbell Plateau (New Zealand) - Report of the RV SONNE cruise SO-169, Projekt CAMP, 17 January to 24 February 2003. Bremerhaven: Alfred-Wegener-Institut für Polar- und Meeresforschungpp. (Berichte zur Polar- und Meeresforschung; 457).

Goto, S., Matsubayashi, O., & Nagakubo, S. (2016). Simulation of gas hydrate dissociation caused by repeated tectonic uplift events. *Journal of Geophysical Research: Solid Earth*, *121*, 3200–3219. https://doi.org/10.1002/2015JB012711

Hain, M. P., Sigman, D. M., & Haug, G. H. (2014). Distinct roles of the Southern Ocean and North Atlantic in the deglacial atmospheric radiocarbon decline. *Earth and Planetary Science Letters*, *394*, 198–208. https://doi.org/10.1016/j.epsl.2014.03.020

Hillman, J. I. T., Gorman, A. R., & Pecher, I. A. (2015). Geostatistical analysis of seafloor depressions on the southeast margin of New Zealand's South Island—Investigating the impact of dynamic near seafloor processes on geomorphology. *Marine Geology*, *360*, 70–83. https://doi.org/10.1016/j.margeo.2014.11.016

Hovland, M., Gardner, J. V., & Judd, A. G. (2002). The significance of pockmarks to understanding fluid flow processes and geohazards. *Geofluids*, *2*, 127–136.

Hovland, M., & Judd, A. G. (1988). *Seabed Pockmarks and Seepages: Ispact on Geology, Biology A. The Marine Environment*. London: Graham, Trotman.

Hu, R., & Piotrowski, A. M. (2018). Neodymium isotope evidence for glacial-interglacial variability of deepwater transit time in the Pacific Ocean. *Nature Communications*, *9*(1), 4709. https://doi.org/10.1038/s41467-018-07079-z

Huybers, P., & Langmuir, C. H. (2017). Delayed CO2 emissions from mid-ocean ridge volcanism as a possible cause of late-Pleistocene glacial cycles. *Earth and Planetary Science Letters*, *457*, 238–249. https://doi.org/10.1016/j.epsl.2016.09.021

Keigwin, L. D., & Lehman, S. J. (2015). Radiocarbon evidence for a possible abyssal front near 3.1 km in the glacial equatorial Pacific Ocean. *Earth and Planetary Science Letters*, *425*, 93–104. https://doi.org/10.1016/j.epsl.2015.05.025

Klaucke, I., Sarkar, S., Bialas, J., Berndt, C., Dannowski, A., Dumke, I., et al. (2018). Giant depressions on the Chatham Rise offshore New Zealand—Morphology, structure and possible relation to fluid expulsion and bottom currents. *Marine Geology*, *399*, 158–169. https://doi.org/10.1016/j.margeo.2018.02.011

Lowe, D. J., Blaauw, M., Hogg, A. G., & Newnham, R. M. (2013). Ages of 24 widespread tephras erupted since 30,000 years ago in New Zealand, with re-evaluation of the timing and palaeoclimatic implications of the Lateglacial cool episode recorded at Kaipo bog. *Quaternary Science Reviews*, *74*, 170–194. https://doi.org/10.1016/j.quascirev.2012.11.022

Lund, D. C., & Asimow, P. D. (2011). Does sea level influence mid-ocean ridge magmatism on Milankovitch timescales? *Geochemistry, Geophysics, Geosystems*, *12*, Q12009. https://doi.org/10.1029/2011GC003693

Lund, D. C., Asimow, P. D., Farley, K. A., Rooney, T. O., Seeley, E., Jackson, E. W., & Durham, Z. M. (2016). Enhanced East Pacific Rise hydrothermal activity during the last two glacial terminations. *Science*, *351*(6272), 478–482. https://doi.org/10.1126/science.aad4296

Lund, D. C., Mix, A. C., & Southon, J. (2011). Increased ventilation age of the deep northeast Pacific Ocean during the last deglaciation. *Nature Geoscience*, *4*(11), 771–774. https://doi.org/10.1038/ngeo1272

Lupton, J., Butterfield, D., Lilley, M., Evans, L., Nakamura, K. I., Chadwick, W. Jr., et al. (2006). Submarine venting of liquid carbon dioxide on a Mariana Arc volcano. *Geochemistry, Geophysics, Geosystems*, *7*, Q08007. https://doi.org/10.1029/2005gc001152

Mangini, A., Godoy, J. M., Godoy, M. L., Kowsmann, R., Santos, G. M., Ruckelshausen, M., et al. (2010). Deep sea corals off Brazil verify a poorly ventilated Southern Pacific Ocean during H2, H1 and the Younger Dryas. *Earth and Planetary Science Letters*, *293*(3-4), 269–276. https://doi.org/10.1016/j.epsl.2010.02.041

Marchitto, T. M., Lehman, S. J., Ortiz, J. D., Fluckiger, J., & van Geen, A. (2007). Marine radiocarbon evidence for the mechanism of deglacial atmospheric CO_2 rise. *Science*, *316*(5830), 1456–1459. https://doi.org/10.1126/science.1138679

Mariotti, V., Paillard, D., Roche, D., Bouttes, N., & Bopp, L. (2013). Simulated Last Glacial Maximum Δ14Catm and the Deep Glacial Ocean Carbon Reservoir. *Radiocarbon*, *55*(3), 1595–1602. https://doi:10.1017/S0033822200048517

Menviel, L., Spence, P., Yu, J., Chamberlain, M. A., Matear, R. J., Meissner, K. J., & England, M. H. (2018). Southern Hemisphere westerlies as a driver of the early deglacial atmospheric CO_2 rise. *Nature Communications*, *9*(1), 2503. https://doi.org/10.1038/s41467-018-04876-4

Passaro, S., Tamburrino, S., Vallefuoco, M., Tassi, F., Vaselli, O., Giannini, L., et al. (2016). Seafloor doming driven by degassing processes unveils sprouting volcanism in coastal areas. *Scientific Reports*, *6*, 22448. https://doi.org/10.1038/srep22448, https://www.nature.com/articles/srep22448#supplementary-information

Petit, J. R., Jouzel, J., Raynaud, D., Barkov, N. I., Barnola, J. M., Basile, I., et al. (1999). Climate and atmospheric history of the past 420,000 years from the Vostok ice core, Antarctica. *Nature*, *399*(6735), 429–436. https://doi.org/10.1038/20859

Rafter, P. A., Herguera, J.-C., & Southon, J. R. (2018). Extreme lowering of deglacial seawater radiocarbon recorded by both epifaunal and infaunal benthic foraminifera in a wood-dated sediment core. *Climate of the Past*, *14*, 1977. https://doi.org/10.5194/cp-14-1977-2018

Ridgwell, A., Hargreaves, J. C., Edwards, N. R., Annan, J. D., Lenton, T. M., Marsh, R., et al. (2007). Marine geochemical data assimilation in an efficient Earth System Model of global biogeochemical cycling. *Biogeosciences*, *4*(1), 87–104. https://hal.archives-ouvertes.fr/hal-00297599, https://doi.org/10.5194/bg-4-87-2007

Ronge, T. A., Sarnthein, M., Roberts, J., Lamy, F., & Tiedemann, R. (2019). East Pacific Rise Core PS75/059-2: Glacial-to-deglacial stratigraphy revisited. *Paleoceanography and Paleoclimatology*, *34*, 432–435. https://doi.org/10.1029/2019pa003569

Ronge, T. A., Tiedemann, R., Lamy, F., Köhler, P., Alloway, B. V., de Pol-Holz, R., et al. (2016). Radiocarbon constraints on the extent and evolution of the South Pacific glacial carbon pool. *Nature Communications*, *7*(1), 1–12. https://doi.org/10.1038/ncomms11487

Rose, K. A., Sikes, E. L., Guilderson, T. P., Shane, P., Hill, T. M., Zahn, R., & Spero, H. J. (2010). Upper-ocean-to-atmosphere radiocarbon offsets imply fast deglacial carbon dioxide release. *Nature*, *466*(7310), 1093–1097. https://www.nature.com/nature/journal/v466/n7310/abs/nature09288.html#supplementary-information

Shao, J., Stott, L. D., Gray, W. R., Greenop, R., Pecher, I., Neil, H. L., et al. (2019). Atmosphere-ocean CO_2 exchange across the last deglaciation from the boron isotope proxy. *Paleoceanography and Paleoclimatology*. https://doi.org/10.1029/2018PA003498

Sikes, E. L., Allen, K. A., & Lund, D. C. (2017). Enhanced $\delta^{13}C$ and $\delta^{18}O$ differences between the South Atlantic and South Pacific during the last glaciation: The deep gateway hypothesis. *Paleoceanography*, *32*, 1000–1017. https://doi.org/10.1002/2017pa003118

Sikes, E. L., Cook, M. S., & Guilderson, T. P. (2016). Reduced deep ocean ventilation in the Southern Pacific Ocean during the last glaciation persisted into the deglaciation. *Earth and Planetary Science Letters*, *438*, 130–138. https://doi.org/10.1016/j.epsl.2015.12.039

Sikes, E. L., & Guilderson, T. P. (2016). Southwest Pacific Ocean surface reservoir ages since the last glaciation: Circulation insights from multiple-core studies. *Paleoceanography*, *31*, 298–310. https://doi.org/10.1002/2015PA002855

Sikes, E. L., Samson, C. R., Guilderson, T. P., & Howard, W. R. (2000). Old radiocarbon ages in the southwest Pacific Ocean during the last glacial period and deglaciation. *Nature*, *405*(6786), 555–559. https://doi.org/10.1038/35014581

Skinner, L., McCave, I. N., Carter, L., Fallon, S., Scrivner, A. E., & Primeau, F. (2015). Reduced ventilation and enhanced magnitude of the deep Pacific carbon pool during the last glacial period. *Earth and Planetary Science Letters*, *411*, 45–52. https://doi.org/10.1016/j.epsl.2014.11.024

Skinner, L. C., Fallon, S., Waelbroeck, C., Michel, E., & Barker, S. (2010). Ventilation of the deep Southern Ocean and deglacial CO_2 rise. *Science*, *328*(5982), 1147–1151. https://doi.org/10.1126/science.1183627

Somoza, L., León, R., Medialdea, T., Pérez, L. F., González, F. J., & Maldonado, A. (2014). Seafloor mounds, craters and depressions linked to seismic chimneys breaching fossilized diagenetic bottom simulating reflectors in the central and southern Scotia Sea, Antarctica. *Global and Planetary Change*, *123*, 359–373. https://doi.org/10.1016/j.gloplacha.2014.08.004

Stanmore, B. R., & Gilot, P. (2005). Review—Calcination and carbonation of limestone during thermal cycling for CO_2 sequestration. *Fuel Processing Technology*, *86*(16), 1707–1743.

Stott, L., Southon, J., Timmermann, A., & Koutavas, A. (2009). Radiocarbon age anomaly at intermediate water depth in the Pacific Ocean during the last deglaciation. *Paleoceanography*, *24*, PA2223. https://doi.org/10.1029/2008pa001690

Stott, L., & Timmermann, A. (2011). Hypothesized link between glacial/interglacial atmospheric CO_2 cycles and storage/release CO_2-rich fluids from the deep sea. In *Understanding the Causes, Mechanisms and Extent of the Abrupt Climate Change*, *Geophysical Monograph Series*, Washington, DC: American Geophysical Union; 193, 123–128. ISSN 0065-8448. https://doi.org/10.1029/2010GM001052

Stott, L. D., Harazin, K. M., & Quintana Krupinski, N. B. (2019). Hydrothermal carbon release to the ocean and atmosphere from the eastern equatorial Pacific during the last glacial termination. *Environmental Research Letters*, *14*(2), 025007. https://doi.org/10.1088/1748-9326/aafe28

Stuiver, M., & Polach, H. A. (1977). Discussion reporting of ^{14}C data. *Radiocarbon*, *19*(3), 355–363. https://doi.org/10.1017/S0033822200003672

Toggweiler, J. R. (1999). Variation of atmospheric CO_2 by ventilation of the ocean's deepest water. *Paleoceanography*, *14*(5), 571–588. https://doi.org/10.1029/1999PA900033

Waghorn, K. A., Pecher, I., Strachan, L. J., Crutchley, G., Bialas, J., Coffin, R., et al., & SO.226 Scientific Party (2018). Paleo-fluid expulsion and contouritic drift formation on the Chatham Rise, New Zealand. *Basin Research*, *30*(1), 5–19. https://doi.org/10.1111/bre.12237

Wood, R. A., & Herzer, R. H. (1993). The Chatham Rise, New Zealand. In P. F. E. Ballance (Ed.), *South Pacific Sedimentary Basins* (pp. 329–349). Amsterdam: Elsevier.

Zhao, N., Marchal, O., Keigwin, L., Amrhein, D., & Gebbie, G. (2018). A synthesis of deglacial deep-sea radiocarbon records and their (in) consistency with modern ocean ventilation. *Paleoceanography and Paleoclimatology*, *33*, 128–151. https://doi.org/10.1002/2017PA003174